

**Higher correlations, universal distributions, and finite size scaling in the field theory of depinning**Pierre Le Doussal<sup>1</sup> and Kay Jörg Wiese<sup>2</sup><sup>1</sup>*CNRS-Laboratoire de Physique Théorique de l'École Normale Supérieure, 24 rue Lhomond, 75005 Paris, France*<sup>2</sup>*KITP, University of California at Santa Barbara, Santa Barbara, California 93106-4030, USA*

(Received 1 April 2003; published 21 October 2003)

Recently we constructed a renormalizable field theory up to two loops for the quasistatic depinning of elastic manifolds in a disordered environment. Here we explore further properties of the theory. We show how higher correlation functions of the displacement field can be computed. Drastic simplifications occur, unveiling much simpler diagrammatic rules than anticipated. This is applied to the universal scaled width distribution. The expansion in  $d=4-\epsilon$  predicts that the scaled distribution coincides to the lowest orders with the one for a Gaussian theory with propagator  $G(q)=1/q^{d+2\zeta}$ ,  $\zeta$  being the roughness exponent. The deviations from this Gaussian result are small and involve higher correlation functions, which are computed here for different boundary conditions. Other universal quantities are defined and evaluated: We perform a general analysis of the stability of the fixed point. We find that the correction-to-scaling exponent is  $\omega=-\epsilon$  and not  $-\epsilon/3$  as used in the analysis of some simulations. A more detailed study of the upper critical dimension is given, where the roughness of interfaces grows as a power of a logarithm instead of a pure power.

DOI: 10.1103/PhysRevE.68.046118

PACS number(s): 64.60.Ak

**I. INTRODUCTION**

Understanding the behavior of an elastic interface in a random potential is important for many experimental systems, and still offers a considerable theoretical challenge [1–4]. It is expected that below the upper critical dimension  $d_{uc}$ , the interface is pinned by an arbitrarily weak disorder into some rough configurations and that at zero temperature it can acquire a nonzero velocity under an applied force  $f$  only if  $f$  is larger than the depinning threshold  $f_c$ . A functional renormalization group (FRG) method predicts that  $d_{uc}=4$  for the statics [5] and for the simplest universality class, the so-called isotropic depinning [6–8].

There has been recent progress towards a precise description of the depinning transition. From the theory side, the FRG for single-component manifolds, originally studied for one loop in an expansion in  $\epsilon=d_{uc}-d$ , has now been extended to a field theory shown to be renormalizable to two loops. Renormalizable, we recall, means it has a well-defined continuum limit, which is independent of all microscopic details, and thus ensures universality of large scale observables. Presumably there exists a fully renormalizable theory to all orders, with full predictive power [9–11]. From the side of numerics, a powerful algorithm allows us to obtain the configurations at (or just below) depinning with much improved accuracy [12–14]. A reasonable agreement between the two methods was found in a measurement of the roughness exponent  $\zeta$ , especially the clear conclusion that  $\zeta>\epsilon/3$  contrarily to a previous conjecture [7,8] ( $\zeta=\epsilon/3$ ) based on the one-loop analysis.

The field theory of depinning in its present form is unconventional in that one must work with a nonanalytic action. This peculiar feature is an important part of the physics of the problem and is necessary to avoid the so-called dimensional reduction. It makes the perturbation theory superficially “ambiguous.” A nontrivial step taken in Refs. [9–11] to define the theory at  $T=0$  as the limit  $v\rightarrow 0$  of the moving phase was to assume that the interface position is monotonic

in time. This removes the ambiguity and, remarkably, leads to a renormalizable theory to at least two loops [9–11]. This is supported by the “noncrossing theorems” which apply to single-component depinning and, remarkably, is the same property allowing to show ergodicity and to construct an efficient algorithm to find the exact critical configuration at depinning [12,15]. The origin of recent progresses in both numerics and field theory are thus related. Clearly, one would like to test this field theory by calculating more universal measurable quantities and study its properties.

In this paper, we further explore the field theory constructed in Refs. [9–11]. We study displacement correlations of more than two points. We find that these correlations are *static*. Although physically natural, if one wants quasistatic depinning to make sense, this manifests itself through rather nontrivial massive cancellations in the time dependence of multipoint diagrams. We elucidate these cancellations and obtain as a consequence for a large class of diagrams much simpler diagrammatic rules than previously anticipated. Basically, all time integrals become almost trivial, resulting in a theory with “quasistatic” diagrams. We then apply these properties to the calculation of universal observables. One natural universal quantity is the so-called width distribution of the interface. Interestingly, to the two lowest leading orders in  $\epsilon=4-d$ , the distribution coincides with the one for a Gaussian theory with the full nontrivial propagator  $G(q)=1/q^{d+2\zeta}$ ,  $\zeta$  being the depinning exponent. This is also the subject of a related publication [16], where the distribution is also measured numerically. Here we give a detailed presentation and also compute the higher connected cumulants of the displacement field, i.e., deviations from the Gaussian. Some of these results are quoted in Ref. [16].

In the second part, we study the theory at the upper critical dimension. The motivation is that no exact result is available to confirm that  $d_{uc}=4$  (the only exactly solved limit corresponding to fully connected models [17–19]). Thus the question of what is the upper critical dimension  $d_{uc}$  is still debated, even though the field theory of depinning [6–11,20]

clearly predicts  $d_{uc}=4$ . Also, in the other class of depinning transitions, the so-called anisotropic depinning class with Kardar-Parisi-Zhang nonlinearities, there is not even a convincing prediction for  $d_{uc}$  [21–23], and recent numerical studies have reopened the debate [24]. Recently it has become possible to study numerically depinning and statics in high-dimensional spaces for reasonable system sizes with better precision, allowing for the hope to settle the issue of the upper critical dimension in the near future [12–14,25]. It is thus important to give precise predictions for the behavior predicted by the FRG in order to compare with numerics.

Finally, we also clarify the issue of finite-size scaling. In a previous work, used in several simulations, the value  $\omega = -\epsilon/3$  was used for the finite-size scaling exponent [26,27]. We find that the correct value is instead  $\omega = -\epsilon$ . This may prove useful in numerical studies [28].

The paper is organized as follows. In Sec. II, we define the model, briefly review the FRG method and field theory and define the main observable of interest here, the width distribution. In Sec. III, we compute the Laplace transform of the width distribution in perturbation theory and find that to lowest order in  $\epsilon$  it coincides with a Gaussian approximation. This approximation is introduced and further studied. Some results on Laplace inversion are given. In Sec. IV, we go beyond the Gaussian approximation and compute higher connected cumulants. The detailed calculation of the fourth cumulant (4-point connected correlation function of the displacement field) is given, and the cancellations that occur in the field theory are studied. In Sec. VI, we discuss the upper critical dimension, and in Sec. VII the finite-size scaling. The effect of various boundary conditions is studied in the Appendix.

## II. MODEL AND OBSERVABLES

### A. Model

We study the overdamped dynamics described by the equation of motion

$$\eta \partial_t u_{xt} = c \nabla_x^2 u_{xt} + F(x, u_{xt}) + f, \quad (1)$$

with friction  $\eta$ . Long-range elasticity relevant for solid friction at the upper critical dimension  $d=2$  can be studied by replacing  $cq^2 \rightarrow c|q|$ . In presence of an applied force  $f$ , the center of mass velocity is  $v = L^{-d} \int_x \partial_t u_{xt}$ . The pinning force is  $F(u, x) = -\partial_u V(u, x)$  and thus the second cumulant of the force is

$$\overline{F(x, u)F(x', u')} = \Delta(u - u') \delta^d(x - x'), \quad (2)$$

such that  $\Delta(u) = -R''(u)$  in the bare model, where  $R(u)$  is the correlator of the random potential. Random bond disorder is modeled by a short-range function  $R(u)$ , random field (RF) disorder of amplitude  $\sigma$  by  $R(u) \sim -\sigma|u|$  at large  $u$ , and charge-density wave (CDW) disorder by a periodic function  $R(u)$ .

### B. Review of FRG and field theory

Let us briefly review the field theoretic approach, more details can be found in Ref. [10]. The dynamical action (Martin-Siggia-Rose) averaged over disorder is given by  $e^{-\mathcal{S}}$  with

$$\mathcal{S}[u, \hat{u}] = \int_{xt} \hat{u}_{xt} (\partial_t - \nabla_x^2) u_{xt} - \frac{1}{2} \int_{xtt'} \hat{u}_{xt} \Delta(u_{xt} - u_{xt'}) \hat{u}_{xt'}. \quad (3)$$

Here and below we denote  $\int_x := \int d^d x$ , in Fourier  $\int_k := \int d^d k / (2\pi)^d$  and  $\int_t = \int dt$ . The FRG shows that the full function  $\Delta(u)$  becomes relevant below  $d = d_{uc} = 4$  and a flow equation for its scale dependence has been derived for one and two loops, in an expansion in  $d = 4 - \epsilon$ . In Ref. [10], this was derived by adding a small mass  $m$  as an infrared cutoff and computing the flow of disorder, defined from the effective action  $\Gamma[u, \hat{u}]$  of the theory, as  $m$  decreases towards zero. As in Ref. [10] we will denote by  $\Delta_0(u)$  the bare disorder correlator, i.e., the one appearing in the action  $\mathcal{S}$  in Eq. (3), and by  $\Delta(u)$  the renormalized one, appearing in  $\Gamma[u, \hat{u}]$  which has a similar expression as in Eq. (3). The rescaled disorder is then defined by

$$\Delta(u) = \frac{1}{\epsilon \tilde{I}_1} m^{\epsilon - 2\zeta} \tilde{\Delta}(um^\zeta), \quad (4)$$

where  $I_1 = m^{-\epsilon} \tilde{I}_1 = \int_k (k^2 + m^2)^{-2}$  is the one-loop integral. It was then shown in Refs. [9,10] that Eq. (3) leads to a functional renormalization group equation

$$\begin{aligned} -m \partial_m \tilde{\Delta}(u) &= (\epsilon - 2\zeta) \tilde{\Delta}(u) + \zeta u \tilde{\Delta}'(u) \\ &\quad - \frac{1}{2} [(\tilde{\Delta}(u) - \tilde{\Delta}(0))^2]'' \\ &\quad + \frac{1}{2} [(\tilde{\Delta}(u) - \tilde{\Delta}(0)) \tilde{\Delta}'(u)^2]'' \\ &\quad + \frac{1}{2} \tilde{\Delta}'(0^+)^2 \tilde{\Delta}''(u) \end{aligned} \quad (5)$$

up to  $O(\Delta^4)$  terms. This equation implies that there are only two main universality classes at depinning, a single RF fixed point for interfaces and a periodic one for CDW type disorder [9,10]. Both  $\zeta$  and the fixed point function  $\tilde{\Delta}^*(u)$  were determined to the order  $O(\epsilon^2)$  for these classes [9,10].

The important feature of the field theory of depinning is that  $\Delta(u)$  has a cusplike nonanalyticity at  $u=0$ . As was shown in Refs. [9,10], calculations in the nonanalytic theory [e.g., yielding Eq. (5)] are meaningfully performed using the expansion

$$\Delta(u) = \Delta(0) + \Delta(0^+) |u| + \frac{1}{2} \Delta(0^+) u^2 + \dots \quad (6)$$

Performing Wick averages yield the usual diagrams, except that their actual values involve averages of, e.g., sign functions of the fields. Replacing everywhere  $\text{sgn}(u_t - u_{t'}) \rightarrow \text{sgn}(t - t')$  is justified for single-component quasistatic de-

pinning (i.e., in the limit of vanishing velocity  $v=0^+$ ). This yields diagrams with sometimes complicated internal time and momentum dependences. We find, however, that in some cases massive cancellations occur despite the complications due to the time dependence between various diagrams, contributing to the same observable.

**C. Universal distributions and observables**

To motivate the present study, let us consider one specific example of a universal observable, the width distribution of the configuration at depinning (the so-called critical configuration). The width of a configuration is defined *in a given disorder realization* as

$$w^2 := \frac{1}{L^d} \int_x (u_x - \bar{u})^2, \tag{7}$$

where  $\bar{u} = (1/L^d) \int_x u_x$  is the center of mass and  $L^d$  is the volume of the system. The basic observation is that the sample to sample probability distribution  $P(w^2)$  of  $w^2$  is expected to be universal, with a single scale set by the disorder averaged second cumulant  $\overline{w^2}$ , i.e.,

$$P(w^2) = \frac{1}{\overline{w^2}} f\left(\frac{w^2}{\overline{w^2}}\right). \tag{8}$$

$f(z)$  is a universal function. This holds for thermal averages in a number of finite temperature problems of pure systems [29–31]. Here we show that it also holds for depinning at  $T=0$  and compute the distribution, first within a simple Gaussian approximation and then within the  $\epsilon$  expansion. In the process we study higher point correlation functions in the field theory of depinning, define specific universal ratios of these (describing deviations from Gaussian behavior), and compute them.

Before turning to actual calculations, let us first summarize the general spirit of the method and discuss the question of the universality of such observables. The hallmark of a renormalizable theory is that if one expresses the correlation functions in an expansion in the *renormalized* disorder  $\Delta$ , then the resulting expressions are UV finite, equivalently they have a well-defined continuum limit, independent of short scale details. On a technical level, this can be achieved by computing correlations in standard perturbation theory to a given order in powers of  $\Delta_0$ , and then using the relation between renormalized disorder  $\Delta$  and the bare one  $\Delta_0$  to the same order, or equivalently through the definition of appropriate counterterms [32]. Here, we restrict ourselves to calculations at dominant order in  $\epsilon$  and thus using either  $\Delta$  or  $\Delta_0$  makes no difference. Beyond the Larkin scale, however, these are nonanalytic functions, which is crucial.

In the limit of large scales or large system sizes, the fixed point form reached by the rescaled  $\Delta$  implies that the resulting observable, e.g., the width distribution, is *universal*. Universal means that these quantities do not depend on the short scale details. However, they *do depend* on the details of the large scale infrared (IR) cutoff, i.e., of the type of chosen

boundary conditions. Here we focus on *periodic boundary conditions* [33], also of interest for numerical simulations [16], although we sometimes give results for other types, for instance for the massive IR cutoff described in the preceding paragraph.

Since the FRG method developed in Refs. [9–11] and summarized above uses a mass as IR cutoff and defines disorder vertices at zero momentum, one should be careful in calculations with, e.g., periodic boundary conditions. Since we only compute observables either to dominant order in  $\epsilon$  or within a one-loop approximation, it is easy to make the necessary replacements, as will be indicated below. For instance, the one-loop FRG equation remains identical to the first two lines of Eq. (5), the only changes being (1)  $-m\partial_m\tilde{\Delta}$  has to be replaced by  $L\partial_L\tilde{\Delta}$ ; (2)  $m \rightarrow 1/L$  in the definition of the rescaled disorder; (3) the one-loop integral  $I_1 = \int_k [1/(k^2 + m^2)^2]$  entering into the definition of the rescaled disorder has to be replaced by its homolog for periodic boundary conditions used below [34]:

$$I_1 := \sum_k \frac{1}{(k^2)^2} \equiv L^{-d} \sum_{n \in \mathbb{Z}^d, n \neq 0} \frac{1}{(2\pi n/L)^4}. \tag{9}$$

**III. WIDTH DISTRIBUTION: PERTURBATION THEORY AND GAUSSIAN APPROXIMATION**

Let us start by giving the simplest approximation for this distribution. It can be derived in two ways: (i) perturbation theory in the renormalized theory to lowest order in  $\epsilon$  (ii) a simple Gaussian approximation. In the end, this will motivate going further, i.e., studying deviations from the Gaussian approximation.

**A. Perturbation theory**

We now study perturbation theory. To compute the width distribution using the dynamical field theoretic method [9,10], one can start from the Laplace transform

$$W(\lambda) = e^{-\lambda w^2} \tag{10}$$

with  $w^2 = \sum_x (u_x - \bar{u})^2$ . Here and below we omit the global multiplicative factor  $L^{-d}$  in the definition of  $w^2$ , since in the end we will always normalize the distribution  $P(w^2)$  by fixing its first moment to unity [in Eq. (10) it can be absorbed by a rescaling of  $\lambda$ ].

Expanding in powers of the correlator of the pinning force  $\Delta(u)$  (to lowest order this is equivalent to  $\Delta_0$ , see above), one finds that to leading order  $\ln W(\lambda)$  is the sum of all connected one-loop diagrams, as represented in Fig. 1. The loop with  $n$  disorder vertices and  $n$  insertions of  $w^2$  is

$$\frac{1}{2n} \sum_q \left( \frac{-2\lambda\Delta(0)}{(q^2)^2} \right)^n. \tag{11}$$

Here and below the sums over  $q$  thus runs over a  $d$ -dimensional hypercubic lattice with spacing  $2\pi/L$ , and the

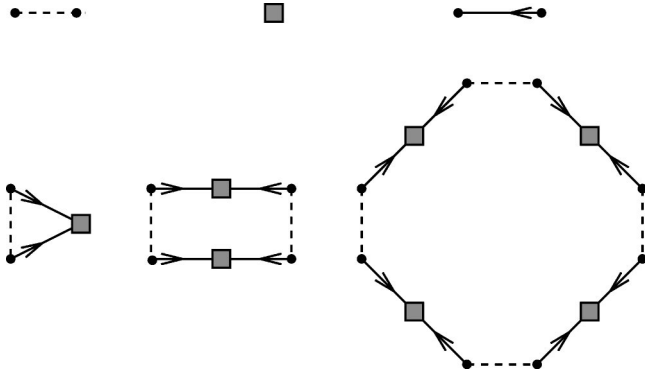


FIG. 1. Examples of contributions to Eq. (10) [terms  $\overline{w^{2c}}$ ,  $\overline{(w^2)^{2c}}$ , and  $\overline{(w^2)^{4c}}$  (bottom)], together with the vertices for disorder (top left),  $w^2$  (top center), and response function (top right).

0 mode is excluded, as appropriate for periodic boundary conditions. If one were now to resum Eq. (11) over  $n$ , one would find

$$W(\lambda) = \prod_q [1 + 2\lambda G(q)]^{-1/2} \quad (12)$$

with  $G(q) = G_{\text{Larkin}}(q) = \Delta(0)/q^4$ , a Larkin model type result if interpreted as naive perturbation theory [i.e., if  $\Delta(0)$  was interpreted as the bare original disorder rather than the renormalized one]. The correct procedure implies that  $\Delta(0)$  is the running renormalized disorder,  $\Delta(0) \rightarrow \Delta_l(0) = (\epsilon \tilde{I}_1)^{-1} e^{(2\xi - \epsilon)l} \tilde{\Delta}^*(0)$ , where  $\tilde{\Delta}^*(0)$  is the (nonuniversal) value of the fixed point [9,10]. Although  $l = \ln(L)$  for the zero momentum disorder vertex, one notes that a momentum  $q$  flows in each vertex and one should take care of this by setting  $l \rightarrow \ln(1/q)$ . This yields finally Eq. (12) with

$$G(q) = C/q^{d+2\xi}, \quad (13)$$

where the value of  $C$  is nonuniversal and fixed by  $\overline{w^2}$ . As will become clear in the following section, the appropriate choice for  $G(q)$  is the two-point finite-size scaling function  $G_L(q) = C/q^{d+2\xi} g(qL)$  with  $g(0) = 1$ . The difference between the two above-mentioned choices for  $l$  simply amounts to the two different limits of small, or large,  $qL$ . However, to lowest order in  $\epsilon = 4 - d$ , they are identical. (For a calculation of the scaling function to next order in  $\epsilon$  see Appendix J in Ref. [10].)

### B. Gaussian approximation and beyond

A more general approach consistent with the previous calculation is the following. We first note that the above result (12) would be exact if the distribution of the displacement fields  $u$  were *Gaussian*. It can thus be called the Gaussian approximation (GA). To understand why it was obtained here, let us consider simply the second connected cumulant of the width distribution  $\overline{(w^2)^2}^c = \overline{(w^2)^2} - \overline{(w^2)}^2$ . This cumulant, however, is not connected with respect to  $u$ , and thus there is an exact relation:

$$\overline{(w^2)^2}^c = \int_{xy} (2G_{xy}^2 + \overline{u_x^2 u_y^2}^c), \quad (14)$$

where here  $G_{xy} = \overline{u_x u_y}$  is the exact disorder averaged two-point function. The first term is just Wick's theorem and would be the full result if the measure of  $u$  were Gaussian. Analogous formulas exist for higher cumulants: the first term on the right-hand side (rhs) of Eq. (14) generalizes into

$$\overline{(w^2)^n}^c |_{\text{GA}} = 2^{n-1} (n-1)! \int_{x_1, \dots, x_n} G_{x_1 x_2} G_{x_2 x_3} \cdots G_{x_n x_1} \quad (15)$$

as a simple consequence of Wick's theorem. This is again easily resummed into Eq. (12) which would thus be exact if the measure of  $u$  were exactly Gaussian. Note that all results of Refs. [29,30] for pure Gaussian theories can also easily be obtained by the present resummation method (temperature replacing disorder). Thus in the GA,  $G(q)$  appearing in Eq. (12) is the exact two-point function. It can be tested in a simulation by inserting the measured two-point function in Eq. (12). In the large but finite system size limit, it takes the scaling function form  $G_L(q)$  discussed above.

When comparing to the numerical results for the width distribution, it turns out that the GA is a surprisingly good approximation even down to  $d = 1$ . This is discussed in detail in Ref. [16]. However, we do not expect the GA to be exact. It is thus interesting to compute the deviation  $D = \int_{xy} \overline{u_x^2 u_y^2}^c$  for the second cumulant of  $w^2$  in Eq. (14). It is computed below and is found to be of order  $\epsilon^4$ , while the GA contribution [first term in Eq. (14)] is of order  $\epsilon^2$  (since  $G \sim \epsilon$ ). Similarly the GA contribution to Eq. (14) is  $O(\epsilon^n)$ , while the deviations are found to be  $O(\epsilon^{2n})$ . This can be summarized as  $u = \sqrt{\epsilon} u_0 + \epsilon u_1$ , where  $u_0$  is a Gaussian random variable of  $O(1)$  and  $u_1$  a non-Gaussian one of  $O(1)$ .

Computing deviations from the GA is thus one motivation to compute higher point correlations.

### C. Laplace inversion

Before doing so, let us discuss how the distribution  $P(w^2)$  is obtained through an inverse Laplace transform as

$$P(w^2) = \oint \frac{d\lambda}{2\pi i} W(\lambda) e^{\lambda w^2}. \quad (16)$$

Noting that in  $d = 1$ , Eq. (12) can also be written as

$$W(\lambda) = \prod_{q>0} [1 + 2\lambda G(q)]^{-1}, \quad (17)$$

this is equivalent to

$$P(w^2) = \sum_{p>0} e^{-[w^2/2G(p)]} \frac{1}{2G(p)} \prod_{q>0, q \neq p} \left[ 1 - \frac{G(q)}{G(p)} \right]^{-1}. \quad (18)$$

This formula shows that for large  $w^2$ , the distribution is dominated by the first term  $p=1$ , and in practice summing the first few terms gives an excellent approximation.

It is instructive to apply Eq. (18) to a random walk, where  $G(q) = 1/q^2$ . Using ( $n \in \mathbb{N}$ )

$$\prod_{n>0} \left( 1 - \frac{x^2}{n^2} \right) = \frac{\sin(\pi x)}{\pi x}, \quad (19)$$

one finds in terms of the width  $\overline{w^2}$

$$P(w^2) = \overline{w^2} \frac{\pi^2}{3} \sum_{n>0} n^2 (-1)^{n+1} e^{-(\pi^2/6)(w^2/\overline{w^2})n^2}. \quad (20)$$

For  $d>1$  the situation is more complicated. Writing

$$P(w^2) = \oint \frac{d\lambda}{2\pi i} e^{w^2\lambda} \prod_{q, q_x > 0} [1 + 2\lambda G(q)]^{-1}, \quad (21)$$

we have, e.g., at least multiplicity  $2d$  for each factor in Eq. (12), as long as no component vanishes, but this multiplicity may even be higher, as can be seen from the following solutions of the diophantic equation (for two dimensions)  $1^2 + 7^2 = 5^2 + 5^2$ ,  $6^2 + 7^2 = 9^2 + 2^2$ , and many more. Let us define the class  $\mathcal{C}(q)$  as

$$p \in \mathcal{C}(q) \quad \text{if} \quad p^2 = q^2. \quad (22)$$

Let us index these classes by  $\alpha$  and introduce an order,

$$\mathcal{C}_\alpha < \mathcal{C}_{\alpha'} \quad \text{if} \quad q \in \mathcal{C}_\alpha \quad \text{and} \quad q' \in \mathcal{C}_{\alpha'} \Rightarrow |q| < |q'|. \quad (23)$$

The number of elements of each class is defined as

$$|\mathcal{C}_\alpha| := \text{number of elements in } \mathcal{C}_\alpha. \quad (24)$$

We further define

$$q_\alpha := \text{any element out of } \mathcal{C}_\alpha. \quad (25)$$

Note that since for  $p \in \mathcal{C}_\alpha$  and  $p \neq 0$  (by definition, we exclude  $p=0$ )  $|\mathcal{C}_\alpha|$  is always even. Equation (21) can then be rewritten as

$$P(w^2) = \oint \frac{d\lambda}{2\pi i} e^{w^2\lambda} \prod_\alpha [1 + 2\lambda G(q_\alpha)]^{-|\mathcal{C}_\alpha|/2}. \quad (26)$$

There are poles at  $\lambda = -[2G(q_\alpha)]^{-1}$ . The sum over these poles can after partial integration be written as

---


$$P(w^2) = \sum_\alpha \frac{1}{(|\mathcal{C}_\alpha|/2 - 1)!} \left( \frac{1}{2G(q_\alpha)} \right)^{|\mathcal{C}_\alpha|/2} \left( \frac{\partial}{\partial \lambda} \right)^{|\mathcal{C}_\alpha|/2 - 1} \left[ e^{w^2\lambda} \prod_{\alpha' \neq \alpha} (1 + 2\lambda G(q_{\alpha'}))^{-|\mathcal{C}_{\alpha'}|/2} \right] \Bigg|_{\lambda = -[2G(q_\alpha)]^{-1}}. \quad (27)$$


---

#### IV. HIGHER POINT CORRELATIONS IN DEPINNING FIELD THEORY

In this section, we analyze how one can compute higher correlations in the depinning field theory and obtain simple diagrammatic rules for doing so. These are illustrated on the four-point function. Specific calculations and results will be given in the following section.

##### A. Preliminaries

We want to compute at  $T=0$ , using the dynamical action  $\mathcal{S}$  in Eq. (3), e.g., the four-point expectation value, connected with respect to disorder (and  $u$ ) as defined in the previous sections:

$$\int_{xy} \overline{u_{xt}^2 u_{yt}^2}^c = \int_{xy} \langle u_{xt}^2 u_{yt}^2 \rangle_c. \quad (28)$$

Similar formulas hold for higher correlation functions. This is identical to a connected expectation value with respect to the action  $\mathcal{S}$ , denoted hereafter as  $\langle \dots \rangle_c$ .

The first step is to show that correlations can all be expressed as

---


$$\langle u_{xt}^2 u_{yt}^2 \rangle_c = \int_{x_i, t_i < t} \mathcal{R}_{x_t, x_1 t_1} \mathcal{R}_{x_t, x_2 t_2} \mathcal{R}_{y_t, x_3 t_3} \mathcal{R}_{y_t, x_4 t_4} \Gamma_{\hat{u}\hat{u}\hat{u}\hat{u}}^{(4)} \times (x_1 t_1, x_2 t_2, x_3 t_3, x_4 t_4). \quad (29)$$


---

Here  $\mathcal{R}$  is the exact response function and  $\Gamma$  is the exact effective action [sum of one-particle irreducible (1PI) graphs] (with the choice  $e^{-\Gamma}$  for the probability and  $\Gamma^{(4)}$  is symmetric). This is the standard relation between connected correlation functions and the effective action [i.e., one-particle irreducible vertex functions (IVF)]. The simplification here is that *a priori* the exact two-point correlation function and vertices such as  $\Gamma_{\hat{u}\hat{u}\hat{u}\hat{u}}^{(4)}$  could also contribute, but their contribution vanishes for  $T=0$  at the depinning threshold. This is because  $\langle u_{xt} u_{x,t_1} \rangle$  is time independent there, and then statistical tilt symmetry implies that all IVF with at least one external  $u$  leg carrying frequency  $\omega$  vanish when this frequency is set to zero (see Sec. II A in Ref. [10]). The above formula (29) generalizes straightforwardly to any connected  $2n$ -point correlation function of the field  $u$  in terms of  $\Gamma_{\hat{u}\dots\hat{u}}^{(2n)}$ .

Next one can compute  $\Gamma_{\hat{u}\hat{u}\hat{u}\hat{u}}^{(4)}$  in perturbation, using the diagrammatic rules for the nonanalytic action arising from

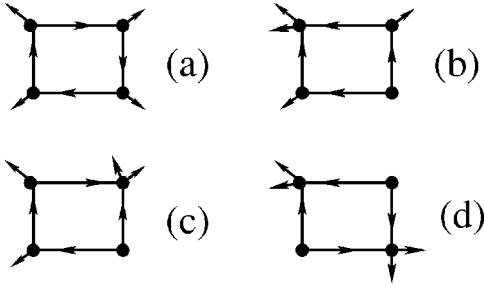


FIG. 2. The four one-loop diagrams with unsplit vertices which contribute to the four-point irreducible vertex function  $\Gamma_{uuuu}^{(4)}$ .

expansion (6). Let us denote  $E_{\hat{u}}$  as the number of  $\hat{u}$  external legs,  $n_v$  as the number of (unsplit) vertices  $\Delta_0$ ,  $n_l$  as the number of internal lines (response functions), and  $L$  as the number of (momentum) loops. Then one has  $2n_v - n_l = E_{\hat{u}}$  and  $L = 1 + n_l - n_v$ . Here one has  $E_{\hat{u}} = 4$  and thus the lowest-order contribution has  $n_v = 4$ ,  $n_l = 4$ , i.e., it is the one-loop square (since two vertices,  $n_v = 2$ , implies  $n_l = 0$  and is disconnected, three vertices,  $n_v = 3$ , implies  $n_l = 2$  and is one-particle reducible). The two-loop corrections are diagrams with five vertices and so on. Similarly  $\Gamma_{\hat{u}\dots\hat{u}}^{(2n)}$  to lowest order is the one-loop  $2n$  polygon diagram.

Since two  $\hat{u}$  fields must come out (arrows) of each vertex, there are four possible diagrams corresponding to the one-loop square, shown in Fig. 2. Each line entering a vertex corresponds to one derivative of the  $\Delta(u)$  function of the vertex. Thus from Eq. (6) we see that diagram (a) is proportional to  $\Delta'(0^+)^4$ , diagrams (b) and (c) to  $\Delta''(0^+)\Delta'(0^+)^2\Delta(0)$ , and diagram (d) to  $\Delta''(0^+)^2\Delta(0)^2$ . However, as we will show below using the so-called mounting property only diagram (a) is nonzero.

We found two ways to compute diagram (a) (as well as any other similar diagram), first a systematic but complicated way, and second a simple way which uses a very important property not yet fully elucidated from the field theory of depinning, the ‘‘quasistatic property’’ described below. To appreciate the extent of the cancellations involved in this drastic simplification, we start by sketching the systematic method.

To perform an actual calculation, since each  $\Delta$  vertex involves fields with two different time arguments, one must switch to the split diagrammatics, as described in Ref. [10]. Diagram (a) of Fig. 2 then becomes the sum of 16 split diagrams (two choices per vertex) represented in Fig. 3. Note that the last one is zero since it involves an acausal loop. That leaves 15 nonzero and nontrivial diagrams.

These diagrams correspond to the following. One first expands  $S^4/4!$  using Eq. (6), which gives schematically

$$\frac{\Delta'(0^+)^4}{2^4 4!} \hat{u}_1 \hat{u}_2 s_{12} u_{12} \hat{u}_3 \hat{u}_4 s_{34} u_{34} \hat{u}_5 \hat{u}_6 s_{56} u_{56} \hat{u}_7 \hat{u}_8 s_{78} u_{78}. \tag{30}$$

In shorthand notation  $\hat{u}_1 = \hat{u}_{x_1, t_1}$ ,  $\hat{u}_2 = \hat{u}_{x_1, t_2}$ ,  $u_{12} = u_1 - u_2$ ,  $s_{12} = \text{sgn}(t_1 - t_2)$ , omitting all space and time integrals. Then carrying the Wick contractions, yielding

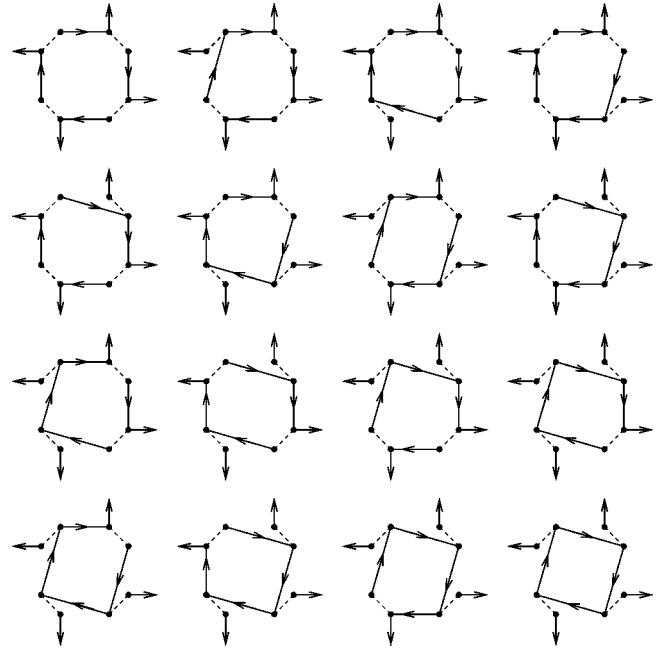


FIG. 3. The 16 one-loop diagrams with split vertices which correspond to diagram (a) in Fig. 2. The last one, which contains an acausal loop and thus vanishes, is added here for future convenience.

$$\frac{\Delta'(0^+)^4}{4!} 2\hat{u}_1 \hat{u}_3 \hat{u}_5 \hat{u}_7 s_{12} s_{34} s_{56} s_{78} (R_{32} - R_{42})(R_{54} - R_{64}) \times (R_{76} - R_{86})(R_{18} - R_{28}); \tag{31}$$

$R_{ij} = \langle \hat{u}_i u_j \rangle$  is the free response function. The factor of 2 comes from the two possible time orientations of the loop. Expanding the product of response functions yields the 16 diagrams represented in Fig. 3, where space and time labels are ordered turning clockwise around the momentum loop. For illustration, let us indicate the full expression of the first diagram in Fig. 3, in momentum space:

$$\Gamma_{(a1)}(p_{12}, t_1; p_{23}, t_3; p_{34}, t_5; p_{41}, t_7) = \Delta'(0^+)^4 \int_{t_2 t_4 t_6 t_8} [\text{sgn}(t_1 - t_2) \text{sgn}(t_3 - t_4) \times \text{sgn}(t_5 - t_6) \text{sgn}(t_7 - t_8) \times R_{p_1, t_3 - t_2} R_{p_2, t_5 - t_4} R_{p_3, t_7 - t_6} R_{p_4, t_1 - t_8}], \tag{32}$$

with  $p_{ij} = p_i - p_j$  the entering momenta and  $R_{p, \tau} = \theta(\tau) e^{-p^2 \tau}$  the free response function. Because of the sgn functions, the evaluation of these integrals and of the other 14 nonvanishing diagrams is very tedious and was handled using MATHEMATICA. Adding all diagrams, massive cancellations occur. The final result is very simple and given below.

Let us now explain the simple method and the properties of the theory which lead to this.

**B. Theorems and other properties**

The simple way to compute the four-point correlations (and higher ones) at depinning is based on the very important following conjectured property.

*Quasistatic property 1.* All correlation functions  $\langle u_{x_1 t_1} \cdots u_{x_{2n} t_{2n}} \rangle$  computed using the diagrammatic rules of the quasistatic field theory of depinning at zero temperature and exactly at threshold are *independent of all time arguments*.

Using relations such as Eq. (29) for arbitrary times shows that an equivalent way to state this property is the following.

*Quasistatic property 2.* All  $\Gamma_{\hat{u} \dots \hat{u}}^{(2n)}(x_1 t_1, \dots, x_{2n} t_{2n})$  are *independent* of  $t_1, \dots, t_{2n}$ .

This property, which appears as a physical requirement for the correct field theory of depinning, implies nontrivial properties of the diagrammatics. Although we will not attempt to prove it here in full generality, we have checked it on many examples, and believe that it works. We encourage the reader to contribute a valid proof. We will, however, state and prove some easier and useful properties below.

Once properties 1 and 2 are accepted, evaluation of the diagrams drastically simplifies, thanks to the following trick. Since the result does not depend on external times, one can take these times mutually infinitely separated, with some fixed (and arbitrary) ordering. Then one can integrate easily over all internal times since the order at each vertex is then specified and each sign function has a fixed value. One recalls that in the splitted diagrammatics all nonvanishing  $T=0$  diagrams are *trees* (see Sec. II A in Ref. [10]). This can be seen on the fifteen nonvanishing diagrams of Fig. 3. Thus integrating independently along each tree starting from the leaves yields one correlation function per link, since  $\int_{t'} R_{q,t-t'} = 1/q^2$ . Performing this calculation on all fifteen diagrams of Fig. 3 shows that they cancel pairwise since they differ only by a global sign, with the exception of the acausal diagram which is zero. Thus the final result is the same as if one had kept only  $(-1)$  times the acausal graph.

Before giving the final result below, let us now state the easier properties.

*Theorem 1 (mounting trick).* A diagram which contributes to an  $u$ -independent vertex function is 0 if it contains a vertex, into which no response function enters.

Examples are diagrams (b), (c), and (d) in Fig. 2. This theorem thus ensures that only diagram (a) is nonvanishing.

*Proof.* The following figure demonstrates the principle. Note that it may be part of a larger diagram. Especially, there may be more response functions entering into the upper disorder. The statement is that

$$\int dt \left( \begin{array}{c} \text{Diagram 1} \\ \text{Diagram 2} \end{array} \right) = 0 . \tag{33}$$

Since no response function enters into the lower disorder  $\Delta(u-u')$ , due to the assumptions this gives  $\Delta(0)$ , with no dependence on time. Thus one can freely integrate over the response function starting at time  $t$ . This integral for both diagrams is  $\int dt R(k,t) = 1/k^2$ . The difference in sign comes from deriving the two different ends of the upper disorder vertex. Thus both contributions exactly cancel.

Thus  $\Gamma_{\hat{u}\hat{u}\hat{u}\hat{u}}^{(4)}(x_1 t_1, x_2 t_2, x_3 t_3, x_4 t_4)$  is given only by diagram (a) in Fig. 2. We have not found a complete proof that it is independent of external times, but we can prove the weaker.

*Lemma 1.* We have

$$\Gamma_{\hat{u}\hat{u}\hat{u}\hat{u}}^{(4)}(x_1 t_1, x_2 t_2, x_3 t_3, x_4 t_4) \tag{34}$$

[see diagram (a) in Fig. 2] is independent of the most-advanced time.

*Proof.* First suppose that a response function enters at the most-advanced time  $t'$ . Then there is the following cancellation:

$$\int dt \left( \begin{array}{c} \text{Diagram 3} \\ \text{Diagram 4} \end{array} \right) = 0 . \tag{35}$$

The mechanism is the same as in the proof of Theorem 1; since by assumption  $t'$  is the most advanced time, the argument of the right-most disorder can never change the sign, and can be integrated over, even though it is odd, i.e.,  $\sim \Delta'(0^+)$ . Thus the remaining diagrams have the structure

$$\begin{array}{c} \text{Diagram 5} \end{array} . \tag{36}$$

This diagram is independent of  $t'$ , as long as  $t'$  is the largest (external) time.

Note that for a loop made out of two disorders, there is only one diagram remaining, namely,

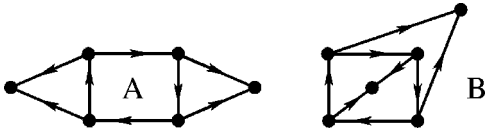
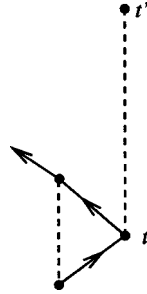


FIG. 4. The two contributions to  $\langle u^4 \rangle_c$  at leading order.



(37)

It is manifestly time independent.  
*Lemma 2.* We have

$$\Gamma_{uuuu}^{(4)}(x_1 t_1, x_2 t_2, x_3 t_3, x_4 t_4) \quad (38)$$

[see diagram (a) in Fig. 2] is independent of the differences in time, if they are very large.

*Proof.* By inspection, one finds that by taking the external times, i.e., one time at each disorder, (infinitely) far apart, the remaining integrals become unambiguous. Thus integrating over the response functions does not leave any time dependence.

As mentioned above, calculation of diagram (a) in Fig. 2 becomes then possible and one finds the following property.

*Property (missing acausal loop).* Diagram (a) in Fig. 2 is given by  $(-1)$  times the acausal loop, if there one replaces each response function by a correlation function.

Intuitively this means that if the acausal loop would give a contribution, then all diagrams would cancel. This seems to be a general mounting theorem.

*Check.* One can calculate diagram (a) in Fig. 4(a) explicitly using none of the above theorems or conjectures. The result is a formidable expression, which has to be integrated over momenta. By evaluating it for given values of the momenta (not even necessarily conserving momentum), one can compare with the prediction of Property 5. We found both expressions to be equal for any randomly chosen values of the momenta. The properties described here suggest the following.

*Property (any loop).* All graphs can be computed to any number of loops, using generalizations of the above rules.

This is not attempted here but preliminary investigation suggests that the same mechanism holds for two loops with some simple end result related to the signs of possible “fermion loops.”

## V. FINAL RESULT FOR THE FOURTH CUMULANT AND UNIVERSAL RATIO

In this section, we compute the fourth cumulant

$$D = \int_{xy} \langle u_{xt}^2 u_{yt}^2 \rangle_c \quad (39)$$

as well as the ratio (kurtosis)

$$R = \frac{D}{2 \int_{xy} G_{xy}^2}, \quad (40)$$

which, according to the discussion in Secs. II and III, is expected to be universal and characterizes the deviations from the Gaussian approximation (for which  $R=0$ ).

Below, we compute  $R$  at depinning both for short-range (respectively, long-range) elasticity to lowest nontrivial order in  $\epsilon=4-d$  (respectively,  $\epsilon=2-d$ ), i.e., within a 1-loop calculation. However, since it turns out that the momentum integrals involved in the calculation depend very strongly on the dimension, we found it useful, and sometimes more accurate, to carry a one-loop approximation directly in fixed dimension  $d$ . Also, since there is one exact result for a massive propagator, we also give the result in that case.

We denote

$$g(q) = \frac{1}{q^2} \quad (41)$$

with the obvious change in the case of long-range elasticity  $g(q) = 1/|q|$ , and (see below) the massive propagator.

The final result in the continuum is given by the sum of the two diagrams in Fig. 4:

$$\begin{aligned} D &= \int_{xy} \langle u_{xt}^2 u_{yt}^2 \rangle_c \\ &= -2\Delta'(0^+)^4 L^d \int \frac{d^d q}{(2\pi)^d} \frac{d^d k}{(2\pi)^d} \frac{d^d p}{(2\pi)^d} \\ &\quad \times [2g(q)^2 g(k)^2 g(p)^2 g(p+q)g(p+k) \\ &\quad + g(q)^2 g(k)^2 g(p)g(p+q)g(p+k)g(p+k+q)], \end{aligned} \quad (42)$$

$$\int_{xy} G_{xy}^2 = L^d \int \frac{d^d q}{(2\pi)^d} G(q)^2 = L^d \Delta(0)^2 \int \frac{d^d q}{(2\pi)^d} g(q)^4. \quad (43)$$

The combinatorics can be done as follows. There is a factor  $1/(4!2^4)$ . There are  $4!$  ways to associate each one of the four external  $u$  to an unsplitted vertex. Say 1,2 are now linked to  $u_x^2$  and 3,4 to  $u_y^2$ . At each vertex, a  $\hat{u}$  field comes out. There are  $2^4$  ways to assign them to each splitted vertex. Then there is a unique set of four splitted points, one at each vertex, entering the acausal graph (which, in effect, is the only one arising with the minus sign). But there are still three ways to join these four points in a loop: Two give the first integral, one the second, and finally for each case the orientation can be chosen in two ways.

Let us go to the discrete model with periodic boundary condition (BC) [33]. We recall that

$$L^d \int \frac{d^d q}{(2\pi)^d} f(q) \equiv \sum_{n \in \mathbb{Z}^d} f\left(\frac{2\pi n}{L}\right), \quad (44)$$

where here and in the following the term with  $n=0$  is always excluded. In the limit of large  $L/a$ , one finds

$$\begin{aligned} D &= a^{2d} \sum_{xy} \langle u_{xt}^2 u_{yt}^2 \rangle_c \\ &= -2\Delta'(0^+)^4 L^{-2d} \left(\frac{L}{2\pi}\right)^{16} \\ &\quad \times \sum_{n,m,l \in \mathbb{Z}^d} \left[ 2 \frac{1}{(n^2)^2 (m^2)^2 (l^2)^2 (l+n)^2 (l+m)^2} \right. \\ &\quad \left. + \frac{1}{(n^2)^2 (m^2)^2 (l^2)^2 (l+n)^2 (l+m)^2 (l+m+n)^2} \right], \end{aligned} \quad (45)$$

$$a^{2d} \sum_{xy} G_{xy}^2 = \Delta(0)^2 \left(\frac{L}{2\pi}\right)^8 \sum_{n \in \mathbb{Z}^d} \frac{1}{n^8}. \quad (46)$$

One can see that the ratio  $R$  will be universal since the one-loop FRG fixed point equation taken at  $u=0$  yields

$$(\epsilon - 2\zeta)\Delta(0) = (\epsilon L)\Delta'(0^+)^2, \quad (47)$$

$$(\epsilon L) = L\partial_L I = \frac{2}{(4\pi)^{d/2} \Gamma\left(3 - \frac{d}{2}\right)} = \frac{1}{8\pi^2}. \quad (48)$$

The last identity is valid for  $d=4$ . In fact, since the one-loop FRG equation is universal, it holds as well for  $d=4$  as for  $d < 4$ . For  $d < 4$ , we use

$$I = \int \frac{d^d p}{(2\pi)^d} \frac{1}{p^4} \equiv L^{-d} \sum_{n \in \mathbb{Z}^d} \frac{1}{(2\pi n/L)^4} = \frac{L^\epsilon}{(2\pi)^4} \sum_{n \in \mathbb{Z}^d} \frac{1}{n^4}, \quad (49)$$

$$L\partial_L I = \epsilon I = \epsilon \frac{L^\epsilon}{(2\pi)^4} \sum_{n \in \mathbb{Z}^d} \frac{1}{n^4}. \quad (50)$$

This is all we need to compute the universal ratio.

#### A. Calculation to lowest order in $\epsilon=4-d$

The ratio  $R = D / (2\sum_{xy} G_{xy}^2)$  is

$$\begin{aligned} R &= -\epsilon^2 (1 - 2\zeta_1)^2 (8\pi^2)^2 \frac{1}{(2\pi)^8} \frac{1}{\sum_{n \in \mathbb{Z}^d} \frac{1}{n^8}} \\ &\quad \times \sum_{n,m,l \in \mathbb{Z}^d} \left[ 2 \frac{1}{(n^2)^2 (m^2)^2 (l^2)^2 (l+n)^2 (l+m)^2} \right. \\ &\quad \left. + \frac{1}{(n^2)^2 (m^2)^2 (l^2)^2 (l+n)^2 (l+m)^2 (l+m+n)^2} \right]. \end{aligned} \quad (51)$$

One finds, using

$$\sum_{n \in \mathbb{Z}} e^{-tn^2} = \Theta(3, 0, e^{-t}) \quad (52)$$

that in  $d=4$

$$\sum_{n \in \mathbb{Z}^d} \frac{1}{n^8} = \frac{1}{6} \int_0^\infty t^3 [\Theta(3, 0, e^{-t})^d - 1] = 10.2454. \quad (53)$$

Noting  $f(p) = \sum_{q \in \mathbb{Z}^d} [1/(q^2)^2 (p+q)^2]$ , one has

$$\begin{aligned} &\sum_{q,k,p \in \mathbb{Z}^d} \frac{1}{(q^2)^2 (k^2)^2 (p^2)^2 (p+k)^2 (p+q)^2} \\ &= \sum_{p \in \mathbb{Z}^d} \frac{1}{(p^2)^2} f(p)^2 \approx 1850, \end{aligned} \quad (54)$$

$$\sum_{n,m,l \in \mathbb{Z}^d} \frac{1}{(n^2)^2 (m^2)^2 (l^2)^2 (l+n)^2 (l+m)^2 (l+m+n)^2} \approx 980. \quad (55)$$

The final result is

$$R = -1.17 \frac{1}{9} \epsilon^2 \approx -0.13 \epsilon^2. \quad (56)$$

This result shows that  $R$  is quite small near  $d=4$ , but increases quite fast as the dimension is lowered. However, the sums over the momenta depend very strongly on  $d$  (see below) and one should expect significant higher-order corrections in  $\epsilon$ . Thus result (56) is likely to drastically overestimate the (absolute value of the) result in lower dimensions, which is why we now turn to an estimate in fixed dimension.

#### B. One-loop estimate in general dimension

One can perform an estimate in general dimension, based on an arbitrary truncation on the (i) one-loop graphs, (ii) neglect of the finite-size scaling function.

In general dimension, one has the dimensionless ratio

$$R = -(\epsilon - 2\zeta)^2 \frac{1}{\left(\epsilon \sum_{n \in \mathbb{Z}^d} \frac{1}{n^4}\right)^2 \sum_{n \in \mathbb{Z}^d} \frac{1}{n^8}}$$

$$\times \sum_{n,m,l \in \mathbb{Z}^d} \left[ \frac{2}{(n^2)^2(m^2)^2(l^2)^2(l+n)^2(l+m)^2} + \frac{1}{(n^2)^2(m^2)^2(l^2)(l+n)^2(l+m)^2(l+m+n)^2} \right]. \quad (57)$$

Let us give a table of values:

$$\sum_{n \in \mathbb{Z}^d} \frac{1}{n^4} = \frac{\pi^4}{45} = 2.164\ 65 \quad (d=1)$$

$$= 6.026\ 812\ 0 \quad (d=2)$$

$$= 16.5 \quad (d=3), \quad (58)$$

$$\sum_{n \in \mathbb{Z}^d} \frac{1}{n^8} = \frac{\pi^8}{4725} = 2.008\ 15 \quad (d=1)$$

$$= 4.281\ 430\ 660\ 805\ 78 \quad (d=2)$$

$$= 6.945\ 807\ 927\ 2 \quad (d=3), \quad (59)$$

$$\sum_{n,m,l \in \mathbb{Z}^d} \frac{1}{(n^2)^2(m^2)^2(l^2)^2(l+n)^2(l+m)^2}$$

$$= 0.373\ 427\ 511\ 17 \quad (d=1)$$

$$= 26.567 \quad (d=2)$$

$$= 240 \quad (d=3), \quad (60)$$

$$\sum_{n,m,l \in \mathbb{Z}^d} \frac{1}{(n^2)^2(m^2)^2(l^2)(l+n)^2(l+m)^2(l+m+n)^2}$$

$$= 0.069\ 672\ 062\ 794\ 960 \quad (d=1)$$

$$= 14.138 \quad (d=2)$$

$$= 143 \quad (d=3). \quad (61)$$

In  $d=1$ , one finds

$$R = -0.086\ 775\ 969\ 128\ 7 \left(1 - 2\frac{\zeta}{\epsilon}\right)^2 \quad (62)$$

$$\approx -0.009\ 641\ 77 \quad (\zeta = \epsilon/3) \quad (63)$$

$$\approx -0.003\ 47 \quad (\zeta = 1.2). \quad (64)$$

In  $d=2$ , one finds

$$R = -0.4326 \left(1 - 2\frac{\zeta}{\epsilon}\right)^2$$

$$\approx -0.0481 \quad (\zeta = \epsilon/3). \quad (65)$$

In  $d=3$ , one finds

$$R = -0.3297 \left(1 - 2\frac{\zeta}{\epsilon}\right)^2$$

$$\approx -0.0366 \quad (\zeta = \epsilon/3), \quad (66)$$

where we have inserted various choices for  $\zeta$  including the one-loop result,  $\zeta = \epsilon/3$ . One finds that already in  $d=3$ , the one-loop approximation is significantly lower than the extrapolation from Eq. (56) as discussed above.

### C. Long-range elasticity in general dimension

For long-range elasticity, the upper critical dimension is  $d_{uc}=2$ . The general expression for  $R$  is

$$R = -(\epsilon - 2\zeta)^2 \frac{1}{\left(\epsilon \sum_{n \in \mathbb{Z}^d} \frac{1}{n^2}\right)^2 \sum_{n \in \mathbb{Z}^d} \frac{1}{n^4}}$$

$$\times \sum_{n,m,l \in \mathbb{Z}^d} \left[ \frac{2}{(n^2)(m^2)(l^2)|l+n||l+m|} + \frac{1}{(n^2)(m^2)|l||l+n||l+m||l+m+n|} \right]. \quad (67)$$

It is interesting to compute  $R$  in  $d=1$ . Using

$$\sum_{n \in \mathbb{Z}} \frac{1}{n^2} = \frac{\pi^2}{3} = 3.289\ 87, \quad (68)$$

$$\sum_{n \in \mathbb{Z}} \frac{1}{n^4} = \frac{\pi^4}{45} = 2.164\ 65, \quad (69)$$

$$\sum_{n,m,l \in \mathbb{Z}} \frac{1}{(n^2)(m^2)(l^2)|l+n||l+m|} = 3.847, \quad (70)$$

$$\sum_{n,m,l \in \mathbb{Z}} \frac{1}{(n^2)(m^2)|l||l+n||l+m||l+m+n|} = 1.934, \quad (71)$$

one finds

$$R = -0.4109 \left(1 - 2\frac{\zeta}{\epsilon}\right)^2$$

$$\approx -0.045\ 66 \quad (\zeta = \epsilon/3). \quad (72)$$

#### D. Long-range epsilon expansion

Similarly, one can perform an expansion in  $\epsilon = 2 - d$ . In  $d = 2$ , one has

$$\epsilon l = 1/(2\pi), \quad (73)$$

$$\sum_{n \in \mathbb{Z}^2} \frac{1}{n^4} = \frac{\pi^4}{45} = 6.026\,812\,0, \quad (74)$$

$$\sum_{n,m,l \in \mathbb{Z}^2} \frac{1}{(n^2)(m^2)(l^2)|l+n||l+m|} = 550 \pm 20, \quad (75)$$

$$\sum_{n,m,l \in \mathbb{Z}^2} \frac{1}{(n^2)(m^2)|l||l+n||l+m||l+m+n|} = 370 \pm 10. \quad (76)$$

This yields

$$\begin{aligned} R = & -\epsilon^2(1-2\zeta_1)^2(2\pi)^2 \frac{1}{(2\pi)^4} \frac{1}{\sum_{n \in \mathbb{Z}^d} \frac{1}{n^4}} \\ & \times \sum_{n,m,l \in \mathbb{Z}^d} \left[ 2 \frac{1}{(n^2)(m^2)(l^2)|l+n||l+m|} \right. \\ & \left. + \frac{1}{(n^2)(m^2)|l||l+n||l+m||l+m+n|} \right]. \quad (77) \end{aligned}$$

The result is

$$R = -6.17 \frac{1}{9} \epsilon^2 \approx -0.686 \epsilon^2 \quad (78)$$

again, a probable overestimation of the result if naively extrapolated to  $d = 1$ .

#### E. Harmonic well, short-range elasticity

It is interesting to compare with the calculation in a massive scheme, i.e., an interface in a harmonic well. Setting  $g(q) := 1/(1+q^2)$ , we have for  $d = 1$ :

$$\int_q g(q)^2 = \frac{\pi}{2} = 1.5708, \quad (79)$$

$$\int_q g(q)^4 = \frac{5\pi}{16} = 1.625\,96, \quad (80)$$

$$\begin{aligned} & \int_q \int_k \int_p g(q)^2 g(k)^2 g(p)^2 g(p+q) g(p+k) \\ & = \frac{1631\pi^3}{31\,104} \\ & = 1.625\,88, \quad (81) \end{aligned}$$

$$\begin{aligned} & \int_q \int_k \int_p g(q)^2 g(k)^2 g(p) g(p+q) g(p+k) g(p+k+q) \\ & = \frac{245\pi^3}{5184} \\ & = 1.465\,38. \quad (82) \end{aligned}$$

This gives the ratio

$$R = -\frac{2366}{1215} (1-2\zeta/\epsilon)^2 = -\frac{2366}{10\,935} = -0.216\,369\,455. \quad (83)$$

It is interesting to compare the present result to one case (to our knowledge, the only one apart from mean field models) where the *full distribution of u* is known in a nontrivial disordered problem [35]. This is the *static* random field model in  $d = 0$  in a harmonic well (i.e., the massive case), the so-called toy model. The exact result there is

$$R_{\text{toy}} = -0.080\,865 \dots \quad (84)$$

The present one-loop approximation for the problem of depinning, continued to  $d = 0$ , would give the larger result  $R = -1/3$ . It is unclear at present whether the difference between the two results indicates that the one-loop approximation is unsatisfactory so far from  $d = 4$ , or if statics and depinning have radically different values of  $R$ .

#### VI. BEHAVIOR AT THE CRITICAL DIMENSION

In this section, we reexamine isotropic depinning, and statics, exactly in  $d = 4$ . We solve the RG equations in  $d = 4$  and obtain the behavior of the correlation function. Contrarily to periodic systems at the upper critical dimension [36], nonperiodic objects such as interfaces submitted to either random bond or random field type disorder exhibit a roughness, which is a power of a logarithm. Note that this conclusion has independently been obtained by Fedorenko and Stepanow [37].

The FRG flow equation ( $\beta$  function) for the (renormalized) force correlator has a good limit for  $d = 4$ . If one defines

$$\Delta_l(u) = 8\pi^2 l^{2\zeta_1 - 1} \tilde{\Delta}_l(u l^{-\zeta_1}) \quad (85)$$

with  $l = \ln(\Lambda/m)$  ( $\Lambda$  some UV cutoff), then the function  $\tilde{\Delta}_l(u)$  satisfies

$$\begin{aligned} \partial_l \tilde{\Delta}(u) = & (1-2\zeta_1) \tilde{\Delta}(u) + \zeta_1 u \tilde{\Delta}'(u) - \frac{1}{2} [(\tilde{\Delta}(u) - \tilde{\Delta}(0))^2]'' \\ & + l^{-1} \beta_2(\tilde{\Delta}), \quad (86) \end{aligned}$$

where, for depinning,

$$\beta_2(\Delta) = [(\Delta(u) - \Delta(0)) \Delta'(u)^2]'' + \Delta'(0^+)^2 \Delta''(u) \quad (87)$$

and  $\zeta_1 = \zeta/\epsilon = 1/3$  is the one-loop value, see e.g., Ref. [10]. It is then easy to see that the function  $\tilde{\Delta}_l(u)$  converges towards the one-loop fixed point with the following asymptotic corrections:

$$\tilde{\Delta}_l(u) = \tilde{\Delta}^*(u) + \sum_n l^{-\omega_n} b_n(u) + \frac{1}{l} \beta'_1[\tilde{\Delta}^*]^{-1} \beta_2(\tilde{\Delta}^*), \quad (88)$$

where  $(\beta'_1)^{-1}$  is the inverse of the linearized one-loop  $\beta$  function and  $\omega_n$  are the one-loop eigenvalues.

Using Eq. (85) with  $\zeta_1 = 1/3$  yields the result for the correlation function at  $q=0$ :

$$\begin{aligned} \langle u_q u_{-q} \rangle |_{q \ll m} &= m^{-4} \Delta(0) \\ &= c m^{-4} \ln(\Lambda/m)^{-1/3} [1 + O(1/\ln(\Lambda/m))] \end{aligned} \quad (89)$$

as  $m \rightarrow 0$ , with  $c = 8\pi^2 \tilde{\Delta}^*(0)$ , both for statics and depinning; the difference lies in the subdominant piece. Within the present approach using the renormalization scheme at  $q=0$ , the two-point correlation function at nonzero  $q$  can be computed from the renormalized (uniform) effective action by resumming an infinite set of diagrams. Using the standard finite-size scaling ansatz allows to obtain the other limit of the scaling function, where  $\Lambda \gg q \gg m$ . To lowest order (one loop) in the renormalized disorder, one has [11]

$$\begin{aligned} (q^2 + m^2)^2 \langle u_q u_{-q} \rangle &= [\Delta(0) - \Delta'(0^+)^2 (I(q) - I(0)) + \dots], \\ I(q) &= \int_p \frac{1}{(p^2 + m^2)((p+q)^2 + m^2)}. \end{aligned} \quad (90)$$

This gives

$$\langle u_q u_{-q} \rangle = c (q^2 + m^2)^{-2} \ln\left(\frac{\Lambda}{m}\right)^{-1/3} \left( 1 - \frac{1}{3} \frac{\ln\left(\frac{m}{q}\right)}{\ln\left(\frac{\Lambda}{m}\right)} + \dots \right). \quad (91)$$

Assuming scaling, i.e., the function  $(1 - \frac{1}{3}x + \dots) \rightarrow (1+x)^{-1/3}$ , one finds

$$\langle u_q u_{-q} \rangle \sim q^{-4} \left[ \ln\left(\frac{m}{q}\right) \right]^{-1/3} \quad (92)$$

and thus

$$\overline{(u_x - u_0)^2} \sim (\ln x)^{2/3}. \quad (93)$$

## VII. STABILITY OF THE ONE-LOOP FIXED POINT

Here we analyze the stability of a functional fixed point. The following two cases have to be distinguished.

(a) There is the freedom to rescale the field  $u$  while, at the same time, rescaling the disorder correlator. This includes the random bond and random field interface models.

(b) There is no such freedom, since the period is fixed by the microscopic disorder. This is the case for a charge-density wave (random periodic problem), also for the random field bulk problem, in its treatment via a nonlinear  $\sigma$  model.

We first analyze the simpler case (b).

### A. Stability of a functional fixed point; periodic case

Let us consider the flow equation given by

$$\partial_l R(u) = \beta[R](u) = \epsilon R(u) + f[R, R](u), \quad (94)$$

where  $f$  is some bilinear form of  $R$ , which contains at least one derivative for each  $R$ . A similar equation of course exists for  $\Delta(u) = -R''(u)$  and the corresponding  $\beta[\Delta](u)$ .

Suppose  $R^*(u)$  is the nontrivial fixed point of order  $\epsilon$ , i.e.,  $\beta[R^*] = 0$ . Two eigenfunctions and eigenvalues above  $R^*(u)$  can be identified: (i) the constant mode  $\delta R(u) = 1$  with eigenvalue  $\epsilon$  (as long as it is permissible physically); (ii) the first subleading eigenfunction  $\delta R(u) = R^*(u)$  with eigenvalue  $-\epsilon$ .

*Proof.* For case (i), we have for  $\kappa \ll 1$ ,

$$\partial_l (R^*(u) + \kappa) = \beta[R^* + \kappa](u) = \epsilon \kappa, \quad (95)$$

since  $f$  does not couple to the constant by assumption. This proves (i).

For case (ii), we have ( $\kappa \ll 1$ ):

$$\begin{aligned} \partial_l (R^*(u) + \kappa R^*(u)) &= \beta[R^*(1 + \kappa)](u) \\ &= \epsilon R^*(u)(1 + \kappa) \\ &\quad + (1 + \kappa)^2 f[R^*, R^*](u). \end{aligned} \quad (96)$$

Subtracting  $\beta[R^*](u) = 0$  on the rhs and expanding for small  $\kappa$  yields

$$\begin{aligned} \partial_l (R^*(u) + \kappa R^*(u)) &= \epsilon \kappa R^*(u) + 2\kappa f[R^*, R^*](u) \\ &= -\epsilon \kappa R^*(u), \end{aligned} \quad (97)$$

where in the last equation we have again used the fixed-point condition  $\beta[R^*](u) = 0$ , i.e.,  $\epsilon R^*(u) + f[R^*, R^*](u) = 0$ , to eliminate  $f[R^*, R^*](u)$ . This proves (ii).

Using the same line of arguments, it is easy to see that when starting from  $R(u) \sim R^*(u)$  with some arbitrary amplitude, the flow is always remaining on the critical manifold spanned by  $R^*(u)$ .

Of course, there are in general more eigenfunctions and eigenvalues. See Ref. [10] for an explicit example.

### B. Perturbations of the fixed point in the presence of the freedom to rescale

We state the following theorem.

*Theorem.* The differential equation of the form

$$-m \partial_m \Delta(u) = \beta[\Delta],$$

$$\beta[\Delta] = (\epsilon - 2\zeta) \Delta(u) + \zeta u \Delta'(u) + f[\Delta, \Delta], \quad (98)$$

where the symmetric functional  $f[\Delta, \Delta]$ , transforms under  $\Delta(u) \rightarrow \kappa^{-2}\Delta(\kappa u)$  in the same way as  $\Delta$ , has the two eigenfunctions and eigenvalues of perturbations around the fixed point  $\beta[\Delta^*]=0$ ,

$$z_0(u) = u\Delta'(u) - 2\Delta(u), \quad (99)$$

$$\lambda_0 = 0, \quad (100)$$

$$z_1(u) = \zeta u\Delta'(u) + (\epsilon - 2\zeta)\Delta(u), \quad (101)$$

$$\lambda_1 = -\epsilon. \quad (102)$$

(We note  $\Delta$  instead of  $\Delta^*$  for the fixed point for simplicity of notations.) Note that the assumptions are satisfied by the 1-loop flow equation (RF case).

*Proof.* Let  $\beta[\Delta](u) = 0$ . Due to the assumptions, for all  $\kappa$ ,

$$\beta[\kappa^{-2}\Delta](\kappa u) = 0. \quad (103)$$

Deriving with respect to  $\kappa$  gives with Eq. (98) at  $\kappa = 1$ ,

$$\begin{aligned} (\epsilon - 2\zeta)[u\Delta'(u) - 2\Delta(u)] + \zeta u[u\Delta'(u) - 2\Delta(u)]' \\ + 2f[\Delta(u), u\Delta'(u) - 2\Delta(u)] = 0. \end{aligned} \quad (104)$$

This is nothing but the eigenvalue equation for the perturbation  $z_0(u)$  about the fixed point  $\beta[\Delta]=0$  and proves the existence of the solution  $z_0(u)$  with eigenvalue  $\lambda_0 = 0$ . Note that this *redundant* operator with eigenvalue 0 persists to all orders in perturbation theory.

Let us turn to the next solution. Multiplying Eq. (104) with  $\zeta$  and adding  $2\epsilon$  times  $\beta[\Delta]=0$  gives

$$\begin{aligned} (\epsilon - 2\zeta)[\zeta u\Delta'(u) + (2\epsilon - 2\zeta)\Delta(u)] + \zeta u[\zeta u\Delta'(u) \\ + (2\epsilon - 2\zeta)\Delta(u)]' \\ + 2f[\Delta(u), \zeta u\Delta'(u) + (\epsilon - 2\zeta)\Delta(u)] = 0, \end{aligned} \quad (105)$$

where we used the bilinearity of  $\Delta(u)$ . Rearranging yields

$$\begin{aligned} (\epsilon - 2\zeta)[\zeta u\Delta'(u) + (\epsilon - 2\zeta)\Delta(u)] + \zeta u[\zeta u\Delta'(u) \\ + (\epsilon - 2\zeta)\Delta(u)]' + 2f[\Delta(u), \zeta u\Delta'(u) \\ + (\epsilon - 2\zeta)\Delta(u)] = -\epsilon[\zeta u\Delta'(u) + (\epsilon - 2\zeta)\Delta(u)]. \end{aligned} \quad (106)$$

This equation is nothing but the eigenvalue equation for the perturbation  $z_1(u) = \zeta u\Delta'(u) + (\epsilon - 2\zeta)\Delta(u)$  about the fixed point  $\beta[\Delta]=0$  with eigenvalue  $\lambda_1 = -\epsilon$ . Q.E.D.

*Remark.* Consider the case of short-range disorder, i.e.,  $\Delta(u)$  falls off rapidly and is monotonic. Usually, the leading fixed-point solution has no knot [no  $u$  such that  $\Delta(u) = 0$ ]. Then  $z_0(u)$  has no knot and  $z_1(u)$  has one knot. Eigenvalues should be ordered (like in quantum mechanics) due to their number of knots. Thus we should have found the two leading solutions for short-range disorder. This is confirmed by the numerical analysis given in the following section.

*Corollary: Random bond case.* The differential equation of the form

$$-m\partial_m R(u) = \beta[R](u),$$

$$\beta[R](u) = (\epsilon - 4\zeta)R(u) + \zeta uR'(u) + f[R, R](u), \quad (107)$$

where the symmetric functional  $f[R, R]$  transforms under  $R(u) \rightarrow \kappa^{-4}R(\kappa u)$  in the same way as  $R$ , has the two eigenfunctions and eigenvalues of perturbations around the fixed point  $\beta[R^*]=0$ ,

$$z_0(u) = uR'(u) - 4R(u), \quad (108)$$

$$\lambda_0 = 0. \quad (109)$$

$$z_1(u) = \zeta uR'(u) + (\epsilon - 4\zeta)R(u), \quad (110)$$

$$\lambda_1 = -\epsilon. \quad (111)$$

Note that the assumptions are satisfied by the 1-loop flow equation (random bond case).

*Proof.* This can either be proven along the same lines as for Eq. (98) or by deriving  $z_0(u)$  and  $z_1(u)$  twice with respect to  $u$  and then using the theorem for the random field case (98).

### C. Numerical analysis of the RF fixed point

We start from the one-loop flow equation

$$\begin{aligned} -m\partial_m \Delta(u) = (\epsilon - 2\zeta)\Delta(u) + \zeta u\Delta'(u) \\ - \frac{1}{2}[(\Delta(u) - \Delta(0))^2]'. \end{aligned} \quad (112)$$

It has the following solution [5,10]:

$$\Delta(u) = \frac{\epsilon}{3}y_1(u),$$

$$y_1(u) - \ln y_1(u) = 1 + \frac{1}{2}u^2. \quad (113)$$

Perturbations around this solution satisfy the differential equation

$$-m\partial_m[\Delta(u) + z(u)] = \lambda\epsilon z(u), \quad (114)$$

$$\begin{aligned} (1 - 3\lambda)z(u) + uz'(u) - [(y_1(u) - y_1(0))(z(u) - z(0))]'' \\ = 0. \end{aligned} \quad (115)$$

In order to have a criterion for the numerical integration, one has to determine the behavior at infinity. Using, for  $u \rightarrow \infty$ ,

$$y_1(u) \approx e^{-1-u^2/2} \quad (116)$$

and assuming exponentially fast decay for  $z(u)$ , one finds that the asymptotic behavior is

$$z(u) \approx z(0) \frac{(u^2 - 1)e^{-1-u^2/2}}{2 + 3\lambda}. \quad (117)$$

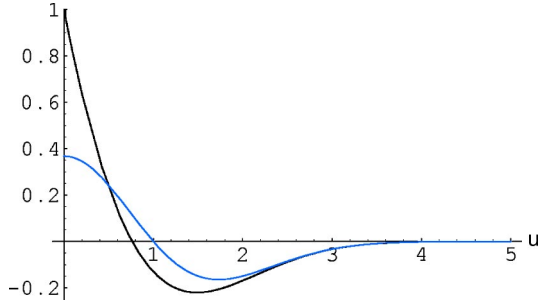


FIG. 5. (Color online) The solution  $z_1(u)$  [in black, with  $z(0) = 1$ ] and asymptotic behavior as given in Eq. (117) (blue/bright).

Quite surprisingly, the asymptotic behavior is fixed, including its amplitude [41]. In any case, slower power law decay is ruled out on a physical ground since we are considering short-range disorder (Fig. 5).

The solutions for  $\lambda = 0$  and  $\lambda = -\epsilon$  are given in Eq. (99) ff. The solution  $z_1(u)$  is dominant, and gives the correction to scaling exponent  $\omega = -\epsilon$ . Note that this exponent is minus the engineering dimension of the coupling, as is the case in standard field theory [38] and also for the random periodic class [10]. Reference [26] cites the value  $\omega = -\epsilon/3$ . We find the corresponding numerical solution to decay as  $u^{-2}$ , incompatible with Eq. (117) and physically unacceptable [38].

The question arises whether there are more solutions with fast decay. Intuitively, one would expect this: Making  $\lambda$  more negative, the solution overshoots and one might think of fine tuning  $\lambda$  such that it approaches the axis for large  $u$  from above. However, this is incompatible with the asymptotic behavior in Eq. (117), which predicts that all solutions for  $\lambda < -2/3$  converge from below. In fact, we have not been able to find any further solution, and we conjecture that there is none. It would be interesting to prove this rigorously. This behavior is in contrast to the random periodic case, solved in Ref. [10], which has infinite many subleading contributions.

### VIII. CONCLUSION

In this paper, we have explored further properties of the field theory of depinning. We have defined and computed universal observables, such as the distribution of the interface width and the ratio  $R$  of the connected four-point cumulant to the square of the two-point one (kurtosis). This ratio measures the deviations from a Gaussian approximation, which we have also used to obtain the universal distribution. Higher-order connected cumulants can be computed in a similar way for one loop using polygon diagrams, and one should be able to reconstruct the full distribution from them. Other properties of the theory such as the behavior at the upper critical dimension and the finite-size scaling behavior have been clarified. All calculations in the present paper are of interest for comparison with numerical simulations, existing ones [16] or in the near future.

In the process of computing the four-point function, we discovered massive cancellations between diagrams. We traced this back to the physically expected property that cor-

relations exactly at depinning should be time independent. A diagrammatic proof of this property is still incomplete, but we have provided some convincing elements in that direction. As a result the correlation functions can be computed in a much simpler way. Thus there seems to be an underlying theory, with “quasistatic” diagrams (i.e., not containing time explicitly), with some additional rules. We have understood these rules to lowest (one-loop) order and it would be of high interest to understand, and prove, them to all orders. It is even possible that there exists a simpler formulation of the theory at depinning in terms of, e.g., effective fermions. The fermionic character is suggested by the cancellation of all diagrams except for the “acausal loops” with a minus sign. We thus encourage further examination of this fascinating question and full elucidation of the field theory which describes depinning.

### APPENDIX: DIFFERENT BOUNDARY CONDITIONS

#### a. Periodic boundary conditions

A periodic function  $u$  with period  $L$  satisfies

$$u(x + L\hat{e}_i) = u(x), \tag{A1}$$

where  $\hat{e}_i$  are orthonormal. It can be written as

$$u(x) = \sum \tilde{u}_k e^{ikx}, \tag{A2}$$

where summation runs over all  $k$ , such that  $k_i = n_i 2\pi/L$ ,  $n_i \in \mathbb{Z}$ .

#### b. Open boundary conditions

To simplify the notation, we give all formulas for one dimension; generalizations are straightforward.

Suppose the function  $f(x)$  is defined on  $[0, L]$ . Then a function  $g(x)$  can be defined by the following prescription:

$$g(x) = \begin{cases} f(x) & \text{for } 0 \leq x \leq L \\ f(2L-x) & \text{for } L < x \leq 2L; \end{cases} \tag{A3}$$

$g(x)$  can be prolonged to a periodic function with period  $2L$ , i.e.,  $g(x+2L) = g(x)$ , and satisfies by construction in addition

$$g(2L-x) = g(x). \tag{A4}$$

In the basis needed to construct functions with period  $2L$ , we have to restrict ourselves to

$$g(x) = \sum \tilde{g}_n \cos\left(\frac{2\pi nx}{2L}\right) = \sum \tilde{g}_n \cos\left(\frac{\pi nx}{L}\right), \tag{A5}$$

since the sine functions do not satisfy Eq. (A4). The such constructed set of functions  $f(x)$ ,  $x \in [0, L]$  has Neumann-boundary conditions at  $x=0$  and  $x=L$ . From Eq. (A5), we infer that the number of modes is reduced by a factor of 2 (compared to the case of closed boundary conditions), but the construction does not change any observable constructed

from  $w^2$  or any energy, all based on the symmetry relation (A4). Importantly, the modes have all mean 0, which is not the case for other basis, e.g., when using antiperiodic functions. Also note that this ansatz reproduces the formula in Ref. [39]. As an interesting consequence, we observe that the following systems lead to the same distribution: (a) an elastic object with  $N$  degrees of freedom, and closed boundary conditions; (b) an elastic object with  $2N$  degrees of freedom, and open boundary conditions.

The simplest example is a one-dimensional random walk

with closed boundary conditions, and a two-dimensional random walk with open boundary conditions, which can be checked numerically [40].

#### ACKNOWLEDGMENTS

We are grateful to W. Krauth and A. Rosso for ongoing collaboration and numerous stimulating discussions, and thank E. Brézin, O. Narayan, and J. M. Schwarz for very useful remarks.

- 
- [1] A.P. Young, *Spin Glasses and Random Fields* (World Scientific, Singapore, 1997).
- [2] M. Kardar, Phys. Rep. **301**, 85 (1998).
- [3] D.S. Fisher, Phys. Rep. **301**, 113 (1998).
- [4] G. Blatter, M.V. Feigel'man, V.B. Geshkenbein, A.I. Larkin, and V.M. Vinokur, Rev. Mod. Phys. **66**, 1125 (1994).
- [5] D.S. Fisher, Phys. Rev. Lett. **56**, 1964 (1986).
- [6] T. Nattermann, S. Stepanow, L.-H. Tang, and H. Leschhorn, J. Phys. II **2**, 1483 (1992).
- [7] O. Narayan and D.S. Fisher, Phys. Rev. B **46**, 11 520 (1992).
- [8] O. Narayan and D.S. Fisher, Phys. Rev. B **48**, 7030 (1993).
- [9] P. Chauve, P. Le Doussal, and K.J. Wiese, Phys. Rev. Lett. **86**, 1785 (2001).
- [10] P. Le Doussal, K.J. Wiese, and P. Chauve, Phys. Rev. B **66**, 174201 (2002).
- [11] P. Le Doussal, K. J. Wiese, and P. Chauve, e-print cond-mat/0304614.
- [12] A. Rosso and W. Krauth, Phys. Rev. B **65**, 012202 (2001).
- [13] A. Rosso and W. Krauth, Phys. Rev. Lett. **87**, 187002 (2001).
- [14] A. Rosso and W. Krauth, Phys. Rev. E **65**, 025101 (2002).
- [15] A. Rosso, These de Doctorat de l'Université Paris VI, Paris, 2002 (unpublished).
- [16] A. Rosso, W. Krauth, P. Le Doussal, J. Vannimenus, and K.J. Wiese, e-print cond-mat/0301464.
- [17] D.S. Fisher, Phys. Rev. B **31**, 1396 (1985).
- [18] D.S. Fisher, Phys. Rev. B **31**, 7233 (1985).
- [19] J. Vannimenus and B. Derrida, J. Stat. Phys. **105**, 1 (2001).
- [20] P. Le Doussal and K.J. Wiese, Phys. Rev. Lett. **89**, 125702 (2002).
- [21] L.-H. Tang, M. Kardar, and D. Dhar, Phys. Rev. Lett. **74**, 920 (1995).
- [22] R. Albert, A.-L. Barabasi, N. Carle, and A. Dougherty, Phys. Rev. Lett. **81**, 2926 (1998).
- [23] P. Le Doussal and K.J. Wiese, Phys. Rev. E **67**, 016121 (2003).
- [24] A. Rosso, A.K. Hartmann, and W. Krauth, Phys. Rev. E **67**, 021602 (2003).
- [25] L. Roters, S. Lübeck, and K.D. Usadel, Phys. Rev. E **66**, 026127 (2002); **66**, 069901 (2002).
- [26] S. Ramanathan and D.S. Fisher, Phys. Rev. B **58**, 6026 (1998).
- [27] J.M. Schwarz and Daniel S. Fisher, Phys. Rev. E **67**, 021603 (2003).
- [28] This has been tested for the data of Ref. [27]. Even though there are no conclusive results,  $\omega = -\epsilon$  is favored over  $\omega = -\epsilon/3$ ; J.M. Schwarz (private communication).
- [29] M. Plischke, Z. Racz, and R.K.P. Zia, Phys. Rev. E **50**, 3589 (1994).
- [30] G. Foltin, K. Oerding, Z. Racz, R.L. Workman, and R.K.P. Zia, Phys. Rev. E **50**, R639 (1994).
- [31] S.T. Bramwell, K. Christensen, J.-Y. Fortin, P.C.W. Holdsworth, H.J. Jensen, S. Lise, J.M. Lopez, M. Nicodemi, J.-F. Pinton, and M. Sellitto, Phys. Rev. Lett. **84**, 3744 (2000).
- [32] A subtle point in that construction is that if one defines  $\Delta_0$  perturbatively from  $\Delta$  to a given order, then  $\Delta_0$  is not the original bare action (which is analytic) thus there is no contradiction in  $\Delta_0$  being nonanalytic. In a sense introducing  $\Delta_0$  is just a trick to express a closed equation for the flow of  $\Delta$  to the same order.
- [33] To be precise, the calculations of this paper assume that the zero mode  $\bar{u}$  is exactly set to zero. In that case momentum sums in internal lines (loops) can exclude  $q=0$  in any diagram. (They are excluded by construction in external lines.) This restriction does not affect the discussion of the GA but is important for the calculations of  $R$  in Sec. IV. The present calculation would apply directly to a numerical simulation, where  $\sum_x u_x = 0$  is enforced in each disorder configuration (pinned zero mode). We will discuss the precise connection between the boundary conditions chosen in simulations such as Ref. [16] and field theoretical calculations in a forthcoming publication.
- [34] To extend the two-loop FRG (5) to that periodic BC scheme, one would have to reevaluate two-loop integrals with discrete sums, or carry other changes in the scheme. This, however, goes beyond the present one-loop study.
- [35] P. Le Doussal and Cecile Monthus, e-print cond-mat/0204168.
- [36] R. Chitra, T. Giamarchi, and P. Le Doussal, Phys. Rev. B **59**, 4058 (1999).
- [37] Andrei A. Fedorenko and Semjon Stepanow, Phys. Rev. E **67**, 057104 (2003).
- [38] J. Zinn-Justin, *Quantum Field Theory and Critical Phenomena* (Oxford University Press, Oxford, 1989).
- [39] T. Antal, M. Droz, G. Gyorgyi, and Z. Racz, Phys. Rev. E **65**, 046140 (2002).
- [40] W. Krauth and A. Rosso (private communication).
- [41] O. Narayan (private communication).